

NANOMATERIALE FOTOLUMINEȘCENTE PE BAZĂ DE HIDROXIAPATITĂ DOPATĂ CU EUROPIU PHOTOLUMINESCENT NANOMATERIALS BASED ON EUROPIUM DOPED HYDROXYAPATITE

ANDREI VIOREL PĂDURARU^{1,2*}, OVIDIU OPREA^{1,2}, ADINA MAGDALENA MUȘUC^{1,3},
BOGDAN ȘTEFAN VASILE^{1,2,4}, ANTON FICAI^{1,2,4,5}, ECATERINA ANDRONESCU^{1,2,4,5}

¹Faculty of Applied Chemistry and Materials Science, Department of Science and Engineering of Oxide Materials and Nanomaterials, University Politehnica of Bucharest, 060042 Bucharest, Romania;

²National Centre for Micro and Nanomaterials, University Politehnica of Bucharest, 060042 Bucharest, Romania

³"Ilie Murgulescu" Institute of Physical Chemistry, Romanian Academy, 060021 Bucharest, Romania;

⁴National Research Center for Food Safety, University Politehnica of Bucharest, 060042 Bucharest, Romania

⁵Academy of Romanian Scientists, 50085 Bucharest, Romania

The paper describes a rapid and a simple method for preparing photoluminescent compounds of different concentration of europium (0-10%) by doping hydroxyapatite, synthesized by coprecipitation method. The obtained nanomaterial were further characterized by Fourier transform infrared spectroscopy, X-ray diffraction analysis, UV-Visible spectroscopy, room-temperature photoluminescence spectroscopy, and scanning electron microscopy. The influence of dopant ion concentration on the structure of hydroxyapatite structure and morphology was followed. Hence, the present study proves the integration of europium ions in hydroxyapatite lattice and an enhanced of the luminescent properties of obtained doped hydroxyapatite materials, even at lower concentrations, being able to extend their applications to bioimaging or drug delivery.

Lucrarea descrie o metodă rapidă și simplă de preparare a compușilor fotoluminescenți cu concentrație diferită de europiu (0-10%) prin doparea hidroxiapatitei, sintetizată prin metoda coprecipitării. Nanomaterialul obținut a fost caracterizat în continuare prin spectroscopie infraroșie transform Fourier, difracției cu raze X, spectroscopie UV-vizibilă, spectroscopie cu fotoluminescență la temperatura camerei și microscopie electronică de scanare. S-a urmărit influența concentrației ionilor dopanți asupra structurii și morfologiei hidroxiapatitei. Prin urmare, studiul de față demonstrează integrarea ionilor de europiu în rețeaua hidroxiapatitei și îmbunătățirea proprietăților fotoluminescente a pulberilor obținute, chiar și la concentrații mai mici, astfel fiind potrivite pentru aplicații în bioimagistica sau la livrarea de medicamente.

Keywords: europium, photoluminescence, hydroxyapatite, coprecipitation

1. Introduction

The progress in nanomaterials science has engendered a wide range of new synthesized compounds using soft and green methodologies, with a great potential for numerous applications. Hydroxyapatite with molecular formula $\text{Ca}_{10}(\text{PO}_4)_6(\text{OH})_2$ (HAp) is a calcium apatite mineral form being the most significant inorganic component of teeth and bones from human body [1, 3]. Numerous studies have shown the synthesis route for HAp in terms of their morphologies (nanorods, plate-like nanocrystals, nanotubes) and functionalities by incorporating different ions. Literature studies were demonstrated the influence of the preparation route on the chemical composition and properties of HAp [4-9]. The hydroxyapatite nanomaterials are currently utilized in numerous applications from bioimaging, biosensing and biomedical field, such as bone repair and regeneration by reason of their analogous chemical compositions of minerals from bones, and, also to its low harmfulness and its biodegradability [10-13].

Recently, the hydroxyapatite nanoparticles doped with various ions have gained attention and become an important scientific domain because of

their improved properties and functions [14-17]. HAp can act as a host matrix due its flexible structure. The ionic substitution of Ca^{2+} , PO_4^- and OH^- ions from HAp lattice can be made using numerous monovalent (K^+ , Ag^+ , Na^+) [18-20] divalent (Zn^{2+} , Sr^{2+} , Mg^{2+} , Cd^{2+} , Cu^{2+}) [21-24], trivalent (Fe^{3+} , Al^{3+} , rare earths ions) [25-26] and tetravalent (Ti^{4+}) [27] cations.

Only several works have reported photoluminescence properties of hydroxyapatite and substituted hydroxyapatite [28-31]. The advantage of substituted hydroxyapatite is superior to undoped one due to the improving photoluminescence properties.

HAp nanoparticles obtained by doping with lanthanide ions will give new properties (for example, luminescence, fluorescent or magnetic ones) and different functions compared with unsubstituted HAp nanomaterials [32]. These new improved materials have been widely studied showing a great potential extended broadly for applications in environmental protection, bioimaging, biosensors, drug delivery, cancer therapy and catalysis [33-38]. The added new properties of lanthanide-doped nanomaterials is to absorb multiple consecutive photons with long lifetime and

* Autor corespondent/Corresponding author,
E-mail: andrei93.paduraru@yahoo.com

stepwise energy levels of trivalent lanthanide ions engrained on this substrate lattice, in order to generate higher energy anti-Stokes luminescence [39].

Among rare earth ions, the most suitable dopant ion for hydroxyapatite is most likely europium (Eu^{3+}) ion, because of its similar ionic radius with Ca^{2+} . Moreover, europium ion exhibits bright green and red-light emission when irradiated with UV light, making it suitable for application in bioimaging and drug delivery systems [40-41].

Herein, it was reported the fruitful synthesis of doped hydroxyapatite nanoparticles with various concentrations of Eu^{3+} prepared by coprecipitation method. The structural, optical and morphological properties of the novel synthesized materials were investigated.

2. Experimental

2.1. Materials

All chemicals were of analytical grade, and they were used without further purification. Calcium nitrate tetrahydrate $\text{Ca}(\text{NO}_3)_2 \cdot 4\text{H}_2\text{O}$, 99.9%, europium-(III) nitrate hexahydrate ($\text{Eu}(\text{NO}_3)_3 \cdot 6\text{H}_2\text{O}$, 99.9%, Alfa Aesar), ammonium phosphate dibasic $[(\text{NH}_4)_2\text{HPO}_4]$, 99.0%, Alfa Aesar), and ammonium hydroxide (NH_4OH , 25% solution) were purchased from Sigma Aldrich, USA. The chemicals were dissolved in deionized water.

2.2. Synthesis procedure

The coprecipitation method was employed to synthesize the europium-doped hydroxyapatite, with chemical formula $(\text{Ca}_{10-x}\text{Eu}_x(\text{PO}_4)_6(\text{OH})_2)$, nanomaterials. The $\text{Ca}_{10-x}\text{Eu}_x(\text{PO}_4)_6(\text{OH})_2$ powders were obtained using the subsequent synthesis procedure. Initially, to the solution obtained by dissolving an amount of $\text{Ca}(\text{NO}_3)_2 \cdot 4\text{H}_2\text{O}$ with different amounts of europium-(III) nitrate hexahydrate in deionized water, while stirring at room temperature, was added dropwise a solution (II) of ammonium phosphate dibasic obtained by dissolving it in deionized water. The solutions were held for 2h under continuous stirring. The pH of the solution was adjusted to 10.5 by using NH_4OH (25%) solution. At the same time, undoped HAp was synthesized using the same method, without the europium precursor chemicals addition. The obtained powder were kept in the solution for maturation, for 24h. Subsequently, the precipitates were filtered off, and washed several times with deionized water until the pH solutions become 7.0 and. The final precipitates were dried at 80°C for 12h, in air oven. In all synthesized powders, the ratio Ca/P and (Ca+Eu)/P was maintained at 1.67.

2.3. Characterization

The obtained nanomaterials were characterized regarding their structural, morphological and optical properties by using

Fourier infrared spectroscopy (FTIR), X-ray diffraction analysis (XRD), scanning electron microscopy (SEM) and UV-Vis and photoluminescence (PL) spectra.

A Fourier infrared FTIR Nicolet iS50R spectrometer, at ambient temperature, in the range 4000–400 cm^{-1} was used. XRD were carried out at room temperature using a PANalytical Empyrean diffractometer with Cu X-ray tube providing a $\text{K}\alpha$ wavelength of 1.541874 Å. The lattice parameters of the sample were refined by the Rietveld method. The size and shape of the particles were evaluated by scanning electron microscopy (SEM) measurements using a Quanta Inspect F50 FEG with 1.2 nm resolution microscope. UV-Vis spectra were recorded on a Able Jasco V-560 spectrophotometer (200 and 850 nm). Photoluminescence (PL) measurements were performed on a Perkin Elmer LS 55 fluorescence spectrophotometer using a 320 nm excitation wavelength.

3. Results and Discussions

3.1. FTIR analysis

FTIR spectra of the $\text{Ca}_{10-x}\text{Eu}_x(\text{PO}_4)_6(\text{OH})_2$ samples (Figure 1) exhibit related profiles and the common absorption bands characteristic for HAp reported in literature [42], proving the presence of pure HAp. The FTIR spectrum of undoped HAp shows a large band which cover 3000 - 3400 cm^{-1} region attributed to adsorbed water. The three bands located around 1090, 1023 and 960 cm^{-1} are specific to the stretching mode of P-O [43]. The adsorption bands around 602 cm^{-1} , 562 cm^{-1} and 474 cm^{-1} are assigned to the bending mode of O-P-O [44]. The presence of a band around 873 cm^{-1} is due to the $[\text{HPO}_4]^{2-}$ ions [45-46].

For all materials, the presence of all above mentioned adsorption bands indicate the occurrence of pure HAp in obtained powders. In all FTIR spectra of $\text{Ca}_{10-x}\text{Eu}_x(\text{PO}_4)_6(\text{OH})_2$ samples, the weak absorption bands which appear around 873 and 1426 cm^{-1} are assigned to CO_3^{2-} probably due to the replacement of the PO_4^{3-} groups, suggesting a reaction between HAp and carbon dioxide from the air [47]. The intensity of phosphate bands decreases with increase of europium concentrations until $x=0.25$, and then the intensity of bands of O-P-O increases. A reason is that the substitution of calcium ions with europium ones induces a modification of bonding forces amongst the ions resulting a weakness of the bands of O-P-O. The increasing in concentration of doping europium ions followed in a reduction of the intensity of this bands, accompanied by a decrease of HAp crystallinity.

3.2. X-ray diffraction analysis

The XRD diffractograms of investigated doped hydroxyapatite, with different europium ion

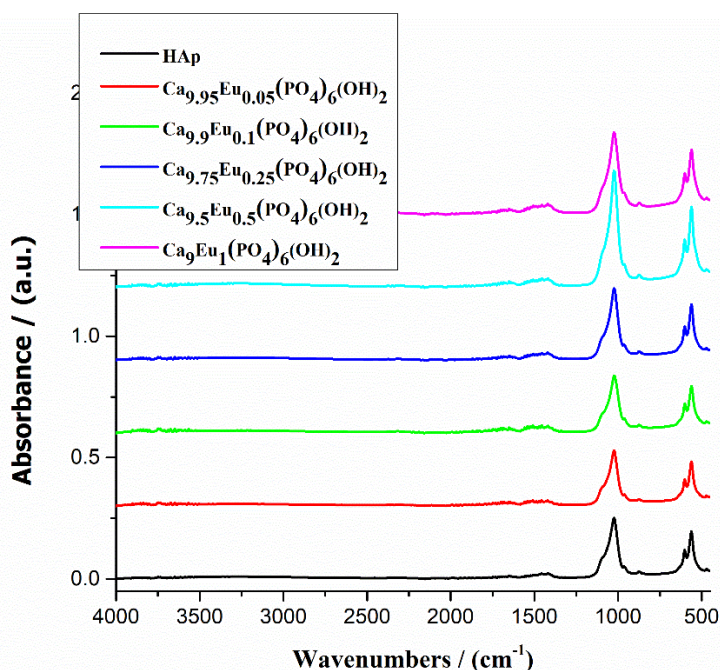


Fig. 1 - FTIR spectra of $\text{Ca}_{10-x}\text{Eu}_x(\text{PO}_4)_6(\text{OH})_2$ samples / Spectre FTIR pentru pulberile de $\text{Ca}_{10-x}\text{Eu}_x(\text{PO}_4)_6(\text{OH})_2$.

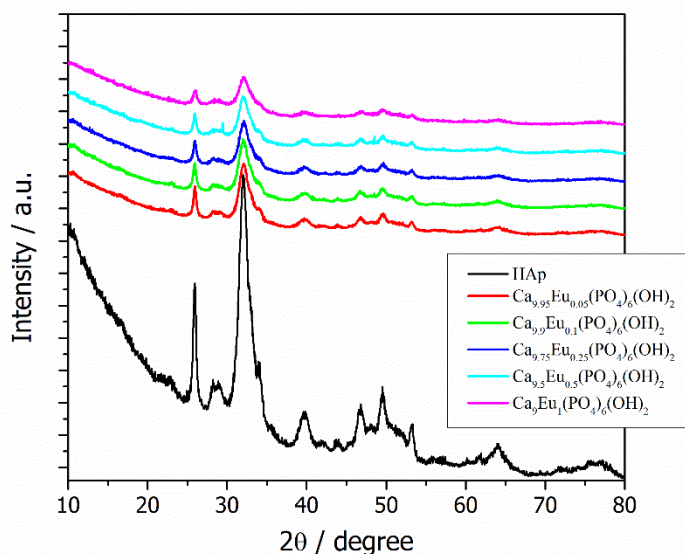


Fig. 2 - XRD analysis of $\text{Ca}_{10-x}\text{Eu}_x(\text{PO}_4)_6(\text{OH})_2$ nanoparticles / Difracție de raze X pentru pulberile de $\text{Ca}_{10-x}\text{Eu}_x(\text{PO}_4)_6(\text{OH})_2$.

concentrations, and the undoped HAp show the formation of a pure hexagonal HAp phase (ICDD PDF4+ card no 00-068-0738, Figure 2) [48], according with literature data [49-51]. The X-ray patterns of the analyzed powders show only the pure hexagonal phase of HAp of with the space group $P6_3/m$, and all diffraction peaks of HAp standard type phase (JCPDS database PDF4+ card no 00-068-0738) such as: (002), (121), (112), (030), (022), (130), (222), (123) and (004).

XRD analysis of $\text{Ca}_{10-x}\text{Eu}_x(\text{PO}_4)_6(\text{OH})_2$ nanoparticles (Figure 2) proves the presence of the major peaks related with 2θ diffraction peaks typical

for a hexagonal lattice structure of HAp. A small shift of the characteristic peaks to higher diffraction angle side can be observed with increasing in concentration of europium ions, ascribed to the substitution of larger size calcium ions (0.099 nm) with smaller size europium ions (0.947Å) [39].

The lattice parameters and the crystallites sizes values of studied samples are gathered in Table 1, and an illustrative variation of those parameters is presented in Figure 3. In all studied samples, the intensities of XRD peaks decrease with the increase of europium ion doping

Table 1

Lattice parameters (crystallite size, D values, lattice microstrains, S and degree of crystallinity χ_c) of synthesized HAp and doped hydroxyapatite using different concentration of europium ions / *Parametri de rețea (dimensiunea de cristalit, tensiunile interne și gradul de cristalinitate) pentru HAp pură și HAp dopată cu concentrații diferite de ioni de europiu*

Samples	D/ nm	S /%	χ_c / %
HAp	6.07±0.82	1.52±0.53	31.50
$\text{Ca}_{10-x}\text{Eu}_x(\text{PO}_4)_6(\text{OH})_2$			
$\text{Ca}_{9.95}\text{Eu}_{0.05}(\text{PO}_4)_6(\text{OH})_2$	5.98±0.73	1.54±0.58	30.19
$\text{Ca}_{9.9}\text{Eu}_{0.1}(\text{PO}_4)_6(\text{OH})_2$	5.55±0.65	1.67±0.62	29.47
$\text{Ca}_{9.75}\text{Eu}_{0.25}(\text{PO}_4)_6(\text{OH})_2$	5.58±0.27	1.66±0.63	26.84
$\text{Ca}_{9.5}\text{Eu}_{0.5}(\text{PO}_4)_6(\text{OH})_2$	5.59±0.67	1.66±0.64	24.94
$\text{Ca}_9\text{Eu}(\text{PO}_4)_6(\text{OH})_2$	4.87±0.34	1.93±0.89	21.70

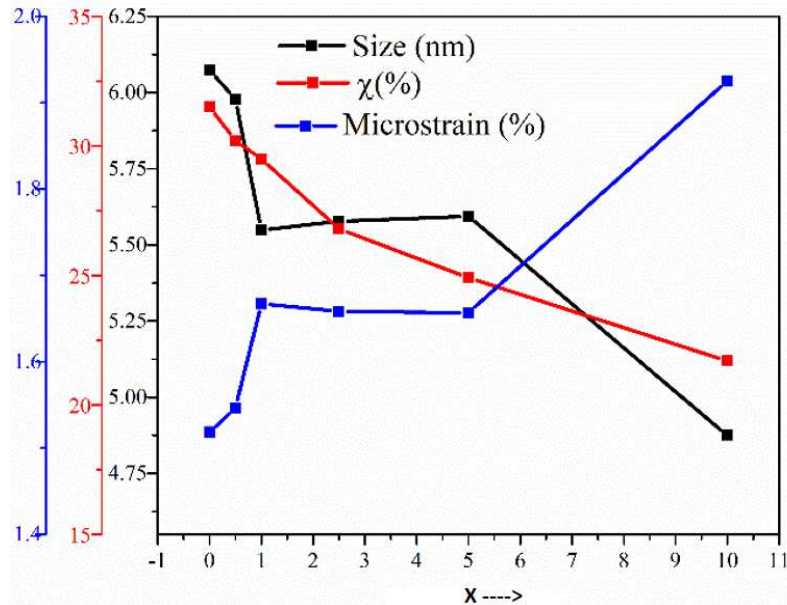


Fig. 3 - The variation of lattice parameters and crystallinity degree with substitution degree for $\text{Ca}_{10-x}\text{Eu}_x(\text{PO}_4)_6(\text{OH})_2$. / *Variația parametrilor de celulă și gradul de cristalinitate cu gradul de substituție pentru pulberile de $\text{Ca}_{10-x}\text{Eu}_x(\text{PO}_4)_6(\text{OH})_2$.*

concentration level, signaling an interference of europium ions with HAp crystal structure.

The calculated average crystallite size of the synthesized hydroxyapatite is of 6.07 nm. In the case of doped nanomaterials was observed a crystallite size decreased with an increase of concentration of dopant ion. Table 2 shows a slowly decrease of the lattice parameters of the europium-doped HAp powders with increasing content of europium. The HAp doping with europium ions induces a decrease of crystallite size from 5.98 to 5.55 nm and an increase of microstrain from 1.54% to 1.67%. Then, for a substitution degree of more than 1%, it was observed a small increase of crystallite size up to 5.59 nm, and subsequently a decrease until 4.87 nm at 10% Eu^{3+} substitution.

The lattice microstrain increase to 1.96% in

the case of maximum substitution degree. The obtained lattice parameters $a=b$ and c of synthesized HAp show the following values: $a=b=9.4227 \text{ \AA}$ and $c=6.8837 \text{ \AA}$, which agree with literature [52, 53]. The small changes in the values of the lattice parameters are assigned to the ionic radius of europium ions (0.947 \AA).

In Table 2 and Figure 4 are shown the unit cell parameters a , c , V and the agreement indices obtained by using the Rietveld analysis (R_{exp} , R_p , R_{wp} and χ^2) indicating the quality of fit, for hydroxyapatite HAp and europium-doped HAp with different concentrations.

The evaluation of crystallinity degree indicates a decrease of crystallinity with increasing ion dopant contents, for all investigated samples.

Table 2

The values of unit cell parameters a , c , V and agreement indices for hydroxyapatite HAp and europium-doped HAp / *Valorile parametrilor celulei elementare a , c , V pentru HAp pură și HAp dopată cu concentrații diferite de ioni de europiu*

Powders	a [Å]	c [Å]	V [Å ³]	R_{exp}	R_p	R_{wp}	χ^2
HAp	9.4227±0.0033	6.8837±0.0025	529.3087	3.1050	4.5059	5.7040	3.3747
$\text{Ca}_{10-x}\text{Eu}_x(\text{PO}_4)_6(\text{OH})_2$							
$\text{Ca}_{9.95}\text{Eu}_{0.05}(\text{PO}_4)_6(\text{OH})_2$	9.4195±0.0036	6.8822±0.0027	528.8417	3.4122	4.5058	5.5556	2.6509
$\text{Ca}_{9.9}\text{Eu}_{0.1}(\text{PO}_4)_6(\text{OH})_2$	9.4253±0.0037	6.8824±0.0029	529.5079	3.3593	4.0399	5.0805	2.2874
$\text{Ca}_{9.75}\text{Eu}_{0.25}(\text{PO}_4)_6(\text{OH})_2$	9.4219±0.00421	6.8821±0.0032	529.1026	3.3522	3.8420	4.7509	2.0086
$\text{Ca}_{9.5}\text{Eu}_{0.5}(\text{PO}_4)_6(\text{OH})_2$	9.4204±0.0051	6.8787±0.0039	528.6695	3.1891	3.9595	4.9234	2.3833
$\text{Ca}_9\text{Eu}(\text{PO}_4)_6(\text{OH})_2$	9.4222±0.0067	6.8727±0.0051	528.4146	3.0222	3.3620	4.0938	1.8348

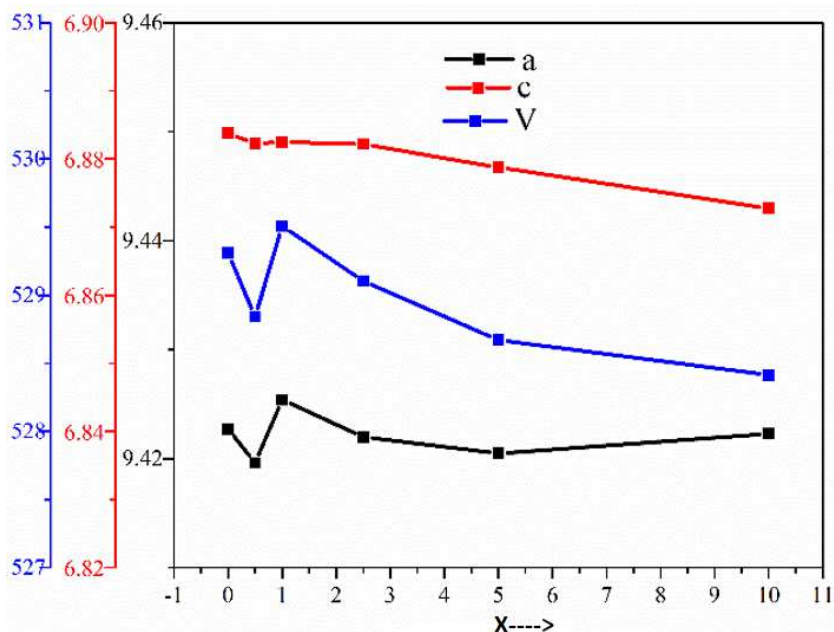


Fig. 4 - Variation of the values of Unit cell parameters with substitution degree for $Ca_{10-x}Eu_x(PO_4)_6(OH)_2$. / Variația valorilor parametrilor celulei elementare cu gradul de substituție pentru pulberile de $Ca_{10-x}Eu_x(PO_4)_6(OH)_2$.

3.3. SEM Analysis

The morphologies of pure HAp and europium doped HAp with five different concentrations were represented in Figures 5 and 6. The scanning electron micrograph of undoped HAp from Figure 5 reveals dense particles with specific morphology of HAp and size between 5-9 nm.

By doping with Eu^{3+} ions, a little influence can be observed in the morphology of substituted

HAp when it was compared with pure HAp. SEM images of Europium doped hydroxyapatite (Figure 6) shows the presence of agglomerates which are present in high density when the concentration of europium ions increases. The shape of particles is quasi-spherical, and the size of particles are found to be in the range of 4-13 nm. From SEM images it was observed that with increase in the europium ions concentration into HAp pattern, the size of particles decreases.

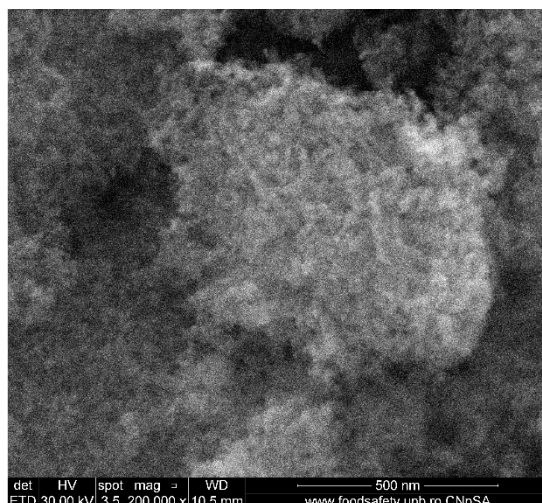


Fig. 5 - The SEM image of undoped HAp / Imagini SEM pentru HAp nedopată.

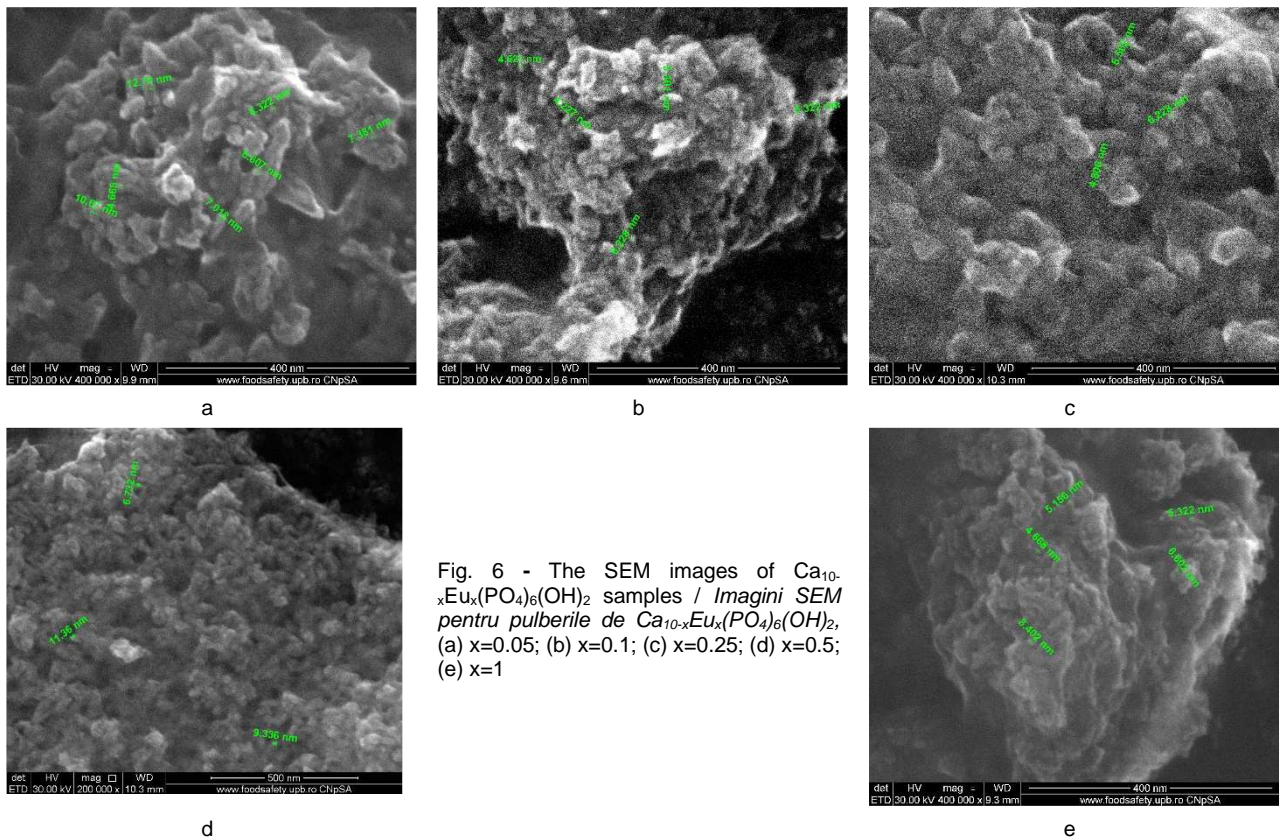


Fig. 6 - The SEM images of $\text{Ca}_{10-x}\text{Eu}_x(\text{PO}_4)_6(\text{OH})_2$ samples / *Imagini SEM pentru pulberile de $\text{Ca}_{10-x}\text{Eu}_x(\text{PO}_4)_6(\text{OH})_2$, (a) x=0.05; (b) x=0.1; (c) x=0.25; (d) x=0.5; (e) x=1*

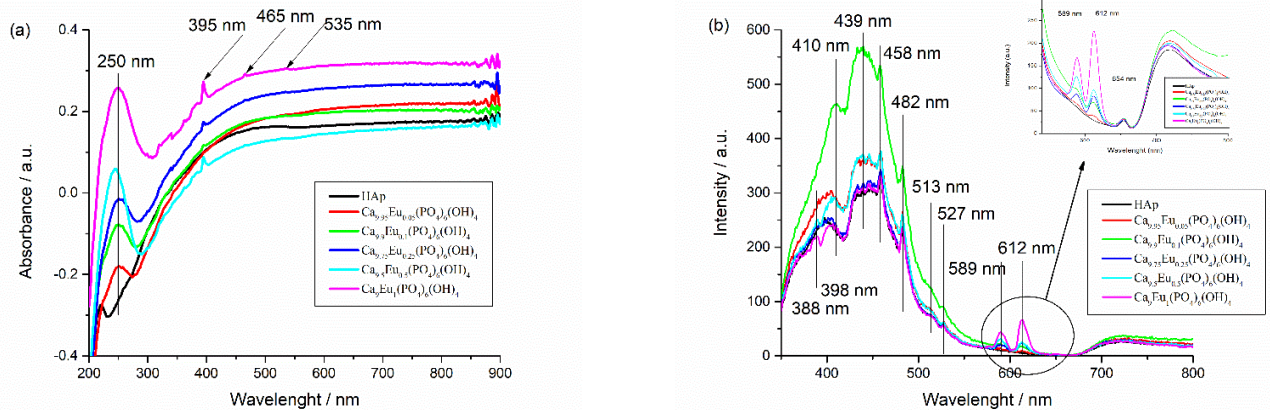


Fig 7- (a) UV-Vis absorption spectra of $\text{Ca}_{10-x}\text{Eu}_x(\text{PO}_4)_6(\text{OH})_2$; (b) PL spectra of $\text{Ca}_{10-x}\text{Eu}_x(\text{PO}_4)_6(\text{OH})_2$ at different concentrations / *(a) Spectre de absorbție UV-Vis (b) Spectre PL pentru pulberile de $\text{Ca}_{10-x}\text{Eu}_x(\text{PO}_4)_6(\text{OH})_2$,*

3.5. UV-Vis and PL Spectra

The absorption spectra of studied powders are presented in Figure 7. A typical tendency was observed for the synthesized compounds. The absorption peaks intensity show an increase and also a broadening with europium concentrations increase.

The UV-Vis spectra of $\text{Ca}_{10-x}\text{Eu}_x(\text{PO}_4)_6(\text{OH})_2$ samples from Figure 7a showed several absorption bands whose intensities increase with increasing europium content: (i) the band at 395 nm corresponds to the ${}^7\text{F}_0 \rightarrow {}^5\text{L}_6$ transition [54], (ii) the band at 465 nm corresponds to the ${}^7\text{F}_0 \rightarrow {}^5\text{D}_2$ transition, and (iii) the other two weak bands at 526 nm assigned to $({}^7\text{F}_0 \rightarrow {}^5\text{D}_1)$ and 535 nm

$({}^7\text{F}_1 \rightarrow {}^5\text{D}_1)$ transitions [55]. The intensities of all absorption bands increase with increasing of europium content.

The PL emission spectra of $\text{Ca}_{10-x}\text{Eu}_x(\text{PO}_4)_6(\text{OH})_2$ samples are presented in Figure 7b. It was observed that the intensity of luminescence of HAp is enhanced by small quantities of europium with a maximum at $x = 0.1$ europium content, and then the intensity decreases with increasing of europium content, the sample with $x = 1$, Eu^{3+} ion presenting a similar fluorescence intensity in domain 350-550 nm as pristine HAp. As a conclusion, the luminescence of HAp samples is enhanced only at small concentration of europium content. Three bands are observed in the emission spectra of europium doped HAp: at 389 nm due to the ${}^7\text{F}_0 \rightarrow {}^5\text{L}_6$

transition, at 512 nm due to the ${}^7F_0 \rightarrow {}^5D_1$ transition and at 526 nm due to the ${}^7F_1 \rightarrow {}^5D_1$ transition. The red fluorescence is indicated by the three emission peaks at 589 nm due to ${}^5D_0 \rightarrow {}^7F_1$ transition; 613 nm due to ${}^5D_0 \rightarrow {}^7F_2$ transition and 654 nm due to ${}^5D_0 \rightarrow {}^7F_3$ transition [56]. The intensities of these three bands are increasing with increasing the europium content in HAp (inset from Figure 7b).

4. Conclusions

In the present research, it has successfully synthesized europium doped hydroxyapatite by coprecipitation method, with chemical formula $\text{Ca}_{10-x}\text{Eu}_x(\text{PO}_4)_6(\text{OH})_4$, where $x = 0.05, 0.1, 0.25, 0.5$ and 1 . The structural characterization by FTIR analysis shows the successful incorporation of europium ion in HAp matrix. The X-ray diffraction analysis confirms that the crystallinity degree, crystallite size and lattice parameters slowly decrease with increasing ion dopant content. The SEM analysis shows the agglomeration nature of nanoparticles and the reducing in their size with increasing of europium ion dopant concentration. From UV-Vis measurements, it was observed an increase of the absorption peaks intensity with increases of europium concentrations. As a conclusion, all samples presented photoluminescent properties but, the photoluminescence of doped HAp powders is enhanced only at small concentration of ions content.

The nanomaterials obtained in the present study based on doped hydroxyapatite with europium ion (3+) in various concentrations, reveal the increases of photoluminescent properties with concentration of dopant ions making them promising candidates for further development and their use for the light emitting capacities. Corroborating the structural, morphological, and optical findings sustain that by coprecipitation method can be obtained new doped hydroxyapatite using different concentrations of europium ion, which can serve as potential nanomaterials with application in imaging or drug delivery systems.

Acknowledgement

The research activity of Andrei Viorel Paduraru was funded by project “: *ExceleŃa academică Ńi valori antreprenoriale - sistem de burse pentru asigurarea oportunităŃilor de formare Ńi dezvoltare a competenŃelor antreprenoriale ale doctoranzilor Ńi postdoctoranzilor – ANTREPENORDOC (36355/23.05.2019 POCU/380/6/13).*

The support from the project “*Innovative biomaterials for treatment and diagnosis, BIONANOINOV grant number PN-III/1-1.2-PCCD-I2017-0629*” is highly appreciated by the rest of the team.

REFERENCES

- [1] S.V. Dorozhkin, M. Epple, Biological and medical significance of calcium phosphates, *Angewandte Chemie International Edition*, 2002, **41**, 3130-3146.
- [2] M. Supova, Substituted hydroxyapatite for biomedical applications: A review, *Ceramics International*, 2015, **41**, 9203-9231.
- [3] G. Gonzalez, C. Costa-Vera, L.J. Borrero, D. Soto, L. Lozada, J. I. Chango, J. C. Diaz, L. Lascano, Effect of carbonates on hydroxyapatite self-activated photoluminescence response, *Journal of Luminescence*, 2018, **195**, 385-395.
- [4] M. Jevtic, M. Mitric, S. Skapin, B. Jancar, N. Ignjatovic, D. Uskokovic, Crystal structure of hydroxyapatite nanorods synthesized by sonochemical homogeneous precipitation, *Crystal Growth & Design*, 2008, **8**, 2217-2222.
- [5] H. B. Zhang, K. C. Zhou, Z. Y. Li, S. P. Huang, Plate-like hydroxyapatite nanoparticles synthesized by the hydrothermal method, *The Journal of Physics and Chemistry of Solids*, 2009, **70**, 243-248.
- [6] C. Lai, S. Q. Tang, Y. J. Wang, K. Wei, Formation of calcium phosphate nanoparticles in reverse microemulsions, *Materials Letters*, 2005, **59**, 210-214.
- [7] K. L. Lin, J. Chang, Y. J. Zhu, W. Wu, G. F. Cheng, Y. Zeng, M. Ruan, A facile one-step surfactant-free and low-temperature hydrothermal method to prepare uniform 3D structured carbonated apatite flowers, *Crystal Growth & Design*, 2009, **9**(1), 177-181.
- [8] M. G. Ma, Y. J. Zhu, J. Chang, Monetite formed in mixed solvents of water and ethylene glycol and its transformation to hydroxyapatite, *The Journal of Physical Chemistry B*, 2006, **110**, 14226-14230.
- [9] F. Chen, Q. L. Tang, Y. J. Zhu, K. W. Wang, M. L. Zhang, W. Y. Zhai, J. Chang, Hydroxyapatite nanorods/poly(vinyl pyrrolidone) composite nanofibers, arrays and three-dimensional fabrics: electrospun preparation and transformation to hydroxyapatite nanostructures, *Acta Biomaterialia*, 2010, **6**, 3013-3020.
- [10] I. R. Mary, S. Sonia, S. Viji, D. Mangalaraj, C. Viswanathan, N. Ponpandian, Novel multiform morphologies of hydroxyapatite: synthesis and growth mechanism, *Applied Surface Science*, 2016, **361**, 25-32.
- [11] R. Bosco, M. Iafisco, A. Tampieri, J. A. Jansen, S.C.G. Leeuwenburgh, J.J.J.P. van den Beucken, Hydroxyapatite nanocrystals functionalized with alendronate as bioactive components for bone implant coatings to decrease osteoclastic activity, *Applied Surface Science*, 2015, **328**, 516-524.
- [12] Y. Yan, X. Zhang, C. Li, Y. Huang, Q. Ding, X. Pang, Preparation and characterization of chitosan-silver hydroxyapatite composite coatings on TiO_2 nanotube for biomedical applications, *Applied Surface Science*, 2015, **332**, 62-69.
- [13] N. Ignjatović, V. Wu, Z. Ajduković, T. Mihajilov-Krstev, V. Uskoković, D. Uskoković, Chitosan-PLGA polymer blends as coatings for hydroxyapatite nanoparticles and their effect on antimicrobial properties, osteoconductivity and regeneration of osseous tissues, *Materials Science and Engineering C: Materials for Biological Applications*, 2016, **60**, 357-364.
- [14] S. Bodhak, S. Bose, A. Bandyopadhyay, Bone cell-material interactions on metal-ion doped polarized hydroxyapatite, *Materials Science and Engineering C: Materials for Biological Applications*, 2011, **31**(4), 755-761.
- [15] T. Iwamoto, Y. Hieda, Y. Kogai, Effect of hydroxyapatite surface morphology on cell adhesion, *Materials Science and Engineering: C*, 2016, **69**, 1263-1267.
- [16] S. Jegatheeswaran, M. Sundarajan, PEGylation of novel hydroxyapatite/PEG/Ag nanocomposite particles to improve its antibacterial efficacy, *Materials Science and Engineering C: Materials for Biological Applications*, 2015, **51**, 174-181.
- [17] Z. Li, E. Ye, David, R. Lakshminarayanan, X. J. Loh, Recent Advances of Using Hybrid Nanocarriers in Remotely Controlled Therapeutic Delivery, *Small*, 2016, **12**(35), 4782-4806.
- [18] H. Li, X. Zhao, S. Cao, K. Li, M. Chen, Z. Xu, J. Lu, L. Zhang, Nd-doped hydroxyapatite coating on carbon/carbon composites: preparation, in vitro bioactivity and biocompatibility, *Applied Surface Science*, 2012, **263**, 163-173.
- [19] S. Kannan, J. M. G. Ventura, J. M. F. Ferreira, Synthesis and thermal stability of potassium substituted hydroxyapatites and hydroxyapatite/ β -tricalciumphosphate mixtures, *Ceramics International*, 2007, **33**, 1489-1494.
- [20] Y. Yan, X. Zhang, Y. Huang, Q. Ding, X. Pang, Antibacterial and bioactivity of silver substituted hydroxyapatite/ TiO_2 nanotube composite coatings on titanium, *Applied Surface Science*, 2014, **314**, 348-357.
- [21] W. Zhang, N. Cao, Y. Chai, X. Xu, Y. Wang, Synthesis of nanosize single-crystal strontium hydroxyapatite via a simple sol-gel method, *Ceramics International*, 2014, **40**, 16061-16064.
- [22] E. S. Thian, T. Konishi, Y. Kawanobe, P. N. Lim, C. Choong, B. Ho, M. Aizawa, Zinc substituted hydroxyapatite: a biomaterial with enhanced bioactivity and antibacterial properties, *Journal of Materials Science: Materials in Medicine*, 2013, **24**, 437-445.
- [23] S. Shanmugam, B. Gopal, Copper substituted hydroxyapatite and fluorapatite: synthesis, characterization and antimicrobial properties, *Ceramics International*, 2014, **40**, 15655-15662.
- [24] V. K. Mishra, B. N. Bhattacharjee, O. Parkash, D. Kumar, S.B. Rai, Mg-doped hydroxyapatite nanoplates for biomedical applications: a surfactant assisted microwave synthesis and spectroscopic investigations, *Journal of Alloys and Compounds*, 2014, **614**, 283-288.
- [25] V. Sarath Chandra, G. Baskar, R. V. Suganthi, K. Elayaraja, M. I. Ahymah Joshy, W. Sofi Beaula, R. Mythili, G. Venkatraman, S. Narayana Kalkura, Blood compatibility of iron-doped nanosize hydroxyapatite and its drug release, *ACS Applied Materials & Interfaces*, 2012, **4**, 1200-1210.

- [26] Y. Nie, C. Hu, C. Kong, Enhanced fluoride adsorption using Al (III) modified calcium hydroxyapatite, *Journal of Hazardous Materials*, 2012, 194-199.
- [27] J. Huang, S. M. Best, W. Bonfield, T. Buckland, Development and characterization of titanium-containing hydroxyapatite for medical applications, *Acta Biomaterialia*, 2010, 6, 241-249.
- [28] T. R. Machado, J. C. Sczancoski, H. Beltran-Mir, I.C. Nogueira, M.S. Li, J. Andres E. Cordoncillo, E. Longo, A novel approach to obtain highly intense self-activated photoluminescence emissions in hydroxyapatite nanoparticles, *Journal of Solid State Chemistry*, 2016, 249, 64-69.
- [29] C. Zhang, J. Yang, Z. Quan, P. Yang, C. Li, Z. Hou, J. Lin, Hydroxyapatite nano- and microcrystals with multiform morphologies: controllable synthesis and luminescence properties, *Crystal Growth & Design*, 2009, 9(6), 2725-2733.
- [30] M. P. Mahabole, M. M. Bahir, N. V Kalyankar, R. S. Khairnar, Effect of incubation in simulated body fluid on dielectric and photoluminescence properties of nano-hydroxyapatite ceramic hopped with strontium ions, *Journal of Biomedical Science and Engineering*, 2012, 5(7), 396-405.
- [31] G. Rosenman, D. Aronov, L. Oster, J. Haddad, G. Mezinskas, I. Pavlovskia, M. Chaikina, A. Karlov, Photoluminescence and surface photovoltage spectroscopy studies of hydroxyapatite nano-bio-ceramics, *Journal of Luminescence*, 2007, 122-123, 936-938.
- [32] C. Heng, X. Zhou, X. Zheng, M. Liu, Y. Wen, H. Houng, D. Fan, J. Hui, X. Zhang, Y. Wei, Surface grafting of rare-earth ions doped hydroxyapatite nanorods (HAp:Ln (Eu/Tb)) with hydrophilic copolymers based on ligand exchange reaction: biological imaging and cancer treatment, *Materials Science and Engineering C: Materials for Biological Applications*, 2018, 91, 556-563.
- [33] C.-L.Tseng, K.-C. Chang, M.-C. Yeh, K.-C. Yang, T.-P. Tang, F.-H. Lin, Development of a dual-functional Pt-Fe-HAP magnetic nanoparticles application for chemo-hyperthermia treatment of cancer, *Ceramics International*, 2014, 40(4), 5117-5127.
- [34] N. Zhang, T. Gao, Y. Wang, Z. Wang, P. Zhang, J. Liu, Environmental pH-controlled loading and release of protein on mesoporous hydroxyapatite nanoparticles for bone tissue engineering, *Materials Science and Engineering C: Materials for Biological Applications*, 2015, 46, 158-165.
- [35] J. Qin, Z. Zhong, J. Ma, Biomimetic synthesis of hybrid hydroxyapatite nanoparticles using nanogel template for controlled release of bovine serum albumin, *Materials Science and Engineering C: Materials for Biological Applications*, 2016, 62, 377-383.
- [36] W. P. S. L. Wijesinghe, M. M. M. G. P. G. Mantilaka, K. G. Chathuranga Senarathna, H. M. T. U., Herath, T. N. Premachandra, C. S. K. Ranasinghe, S. Singh, Preparation of bone-implants by coating hydroxyapatite nanoparticles on self-formed titanium dioxide thin-layers on titanium metal surfaces, *Materials Science and Engineering C: Materials for Biological Applications*, 2016, 63, 172-184.
- [37] Z. Geng, Z. Cui, Z. Li, S. Zhu, Y. Liang, Y. Liu, X. Yang, Strontium incorporation to optimize the antibacterial and biological characteristics of silver-substituted hydroxyapatite coating, *Materials Science and Engineering C: Materials for Biological Applications*, 2016, 58, 467-477.
- [38] G. Zeng, M. Liu, R. Jiang, C. Heng, Q. Huang, L. Mao, Y. Wei, Surface grafting of Eu 3+ doped luminescent hydroxyapatite nanomaterials through metal free light-initiated atom transfer radical polymerization for theranostic applications, *Materials Science and Engineering C: Materials for Biological Applications*, 2017, 77, 420-426.
- [39] S. Mondal, van T. Nguyen, S. Park, J. Choi, L. H. Tran, M. Yi, J. H. Shin, C.-Y. Lee, J. Oh, Bioactive, luminescent erbium-doped hydroxyapatite nanocrystals for biomedical applications, *Ceramics International*, 2020, 46(10)B, 16020-16031.
- [40] F. Chen, P. Huang, Y.-J. Zhu, J. Wu, C.-L. Zhang, D.-X. Cui, The photoluminescence, drug delivery and imaging properties of multifunctional Eu3+/Gd3+ dual-doped hydroxyapatite nanorods, *Biomaterials*, 2011, 32, 9031-9039.
- [41] A. Tesch, C. Wenisch, K.-H. Herrmann, J.R. Reichenbach, P. Warncke, D. Fischer, F.A. Müller, Luminomagnetic Eu3+-and Dy3+-doped hydroxyapatite for multimodal imaging, *Materials Science and Engineering C: Materials for Biological Applications*, 2017, 81, 422-431.
- [42] V. Dhand, K.Y. Rhee, S.-J. Park, The facile and low temperature synthesis of nanophase hydroxyapatite crystals using wet chemistry, *Materials Science and Engineering C: Materials for Biological Applications*, 2014, 36, 152-159.
- [43] Q. Yuan, C. Qin, J. Wu, A. Xu, Z. Zhang, J. Liao, S. Lin, X. Ren, P. Zhang, Synthesis and characterization of Cerium-doped hydroxyapatite/ polylactic acid composite coatings on metal substrates, *Materials Chemistry and Physics*, 2016, 182, 365-371.
- [44] ZUDE FENG, YINGMIN LIAO, MENG YE, Synthesis and structure of cerium-substituted hydroxyapatite, *Journal of materials science: materials in medicine* 2005, 16, 417- 421
- [45] H. Li, X. Sun, Y. Li, B. Li, C. Liang, and H. Wang, "Materials Science & Engineering C Preparation and properties of carbon nanotube (Fe)/ hydroxyapatite composite as magnetic targeted drug delivery carrier," *Mater. Sci. Eng. C*, 2017, 97(December) 222-229, 2019.
- [46] S. Mondal, A. Dey, U. Pal, Low temperature wet-chemical synthesis of spherical hydroxyapatite nanoparticles and their in situ cytotoxicity study, *Adv. Nano. Res.* 2016, 4, 295
- [47] R. Murugan, S. Ramakrishna, Production of ultra-fine bioresorbable carbonated hydroxyapatite, *Acta Biomater.* 2 (2006) 201-206.
- [48] Veselinovic, L., Karanovic, L., Stojanovic, Z., Bracko, I., Markovic, S., Ignjatovic, N., Uskokovic, D. *J. Appl. Crystallogr.* 2010, 43, 320.
- [49] T. A. R. M. Lima and M. E. G. Valerio, "X-ray absorption fine structure spectroscopy and photoluminescence study of multifunctional europium (III)-doped hydroxyapatite in the presence of cationic surfactant medium," *J. Lumin.*, 2018, 201(liv), 70-76.
- [50] J.C. Elliott, *Structure and Chemistry of the Apatites and Other Calcium Orthophosphates*, Elsevier Press, Amsterdam, 1994.
- [51] T. Suzuki, T.Hatsushika, M.Miyake, Synthetic hydroxyapatites as inorganic cation exchangers. Part2 , *J.Chem.Soc., FaradayTrans.*1982, 178, 3605-3611.
- [52] R.V. Gaines, H.C.Skinner, E.E.Foord, B.Mason, A.Rosenzweig, Dana's New Mineralogy, JohnWiley&Sons Inc., NewYork,NY,1997.
- [53] C. Klein, B. Dutrow, *Mineral Science*, John Wiley & Sons Inc., New York, NY, 2008.
- [54] Binnemans, K. Interpretation of europium (III) spectra. *Coord. Chem. Rev.* 2015, 295, 1-45.
- [55] Al-kattan, A.; Dufour, P.; Dexpert-guys, J.; Drouet, C. Preparation and Physicochemical Characteristics of Luminescent Apatite-Based Colloids. 2010, 2918-2924.
- [56] Yang, C.; Yang, P.; Wang, W.; Gai, S.; Wang, J.; Zhang, M.; Lin, J. Synthesis and characterization of Eu-doped hydroxyapatite through a microwave assisted microemulsion process. *Solid State Sci.* 2009, 11, 1923-1928.
